PRELIMINARY REPORT ON THE SOLAR RADIO SPECTROPOLARIMETER IN 2-4 GC/S RANGE

Haruo TANAKA, Takakiyo KAKINUMA, Chikayoshi TORII* and Yoshio TSUKIJI**

Abstract — A solar radio spectropolarimeter for use in 2-4 Gc/s range has been partly completed at Toyokawa. A twin dish receives two linearly polarized components perpendicular to each other, which are changed into right- and left-hand circular components after the frequency is converted by a common swept-frequency local oscillator. Each line is divided into 20 channels corresponding to successive fractions of frequency. Each 20 outputs are swept again and they are added and subtracted for making two outputs corresponding to the swept-frequency signals of intensity and polarization. Additional low-sensitivity channels are working simultaneously. They are recorded on a magnetic tape endlessly until a burst occurs. The signals on the tape are reproduced afterwards one by one and displayed on photographic films. The polarization channel is not yet completed and we are considering to change antenna feeds to receive circularly polarized components directly.

1. Introduction

The properties of solar radio bursts have been extensively studied during this solar cycle by a large amount of observation made all over the world. However, the most remarkable fact which has been found from these observations is that the solar radio bursts are very complicated phenomena which strongly require further interferometric and spectral observations of intensity and polarization over a wide frequency range.

At Toyokawa station, which belongs to the Nagoya University, spectral observations have been made since IGY by combining 4 single frequency observations ranging from 9400 to 1000 Mc/s,(1) associated with 2 interferometers at 9400(2) and 4000(3) Mc/s. From these observations, it has become clear that the radio burst is composed of a few distinctive types even in the microwave frequency range.(4)(5) Especially, there seems to be a clear distinction between the microwave burst and decimeter burst, whose border line usually exists at around 2000-3000 Mc/s. It is the aim of this research project to make clearer the distinction of these burst types. The ability of observing the spectrum of

---

* Contribution to the electronic circuits.

** Contribution to the microwave circuits.

polarization is indispensable for this purpose.

This research project was first planned in 1958 and started construction in 1959. The greater part of the basic experiment and construction had to be made at our institute and about two years had passed before starting observations of intensity spectrum in July 1961. Unfortunately, the sun is becoming more and more quiet, which is really a quite unfavorable situation for the experiment.

2. General Description

2. 1 Antenna Site

After a preliminary experiment of mutual interference with single frequency radiometers, the antenna site was selected as shown in Fig. 1. A small cabin was built close to the antenna where a greater part of the receiver has been put, while the recorder and one of the control panels of the antenna have been placed in the central receiver house.

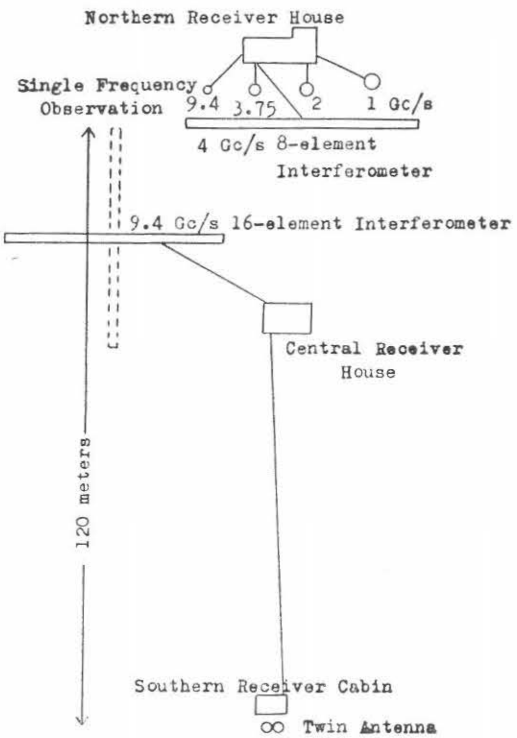

Fig. 1 Plan of the antenna site.

2. 2 Fundamental Principle

The main difference of this system from what has been used at lower frequencies(6) is that this is a multichannel system which is equivalent to 20 radiometers put together into one. This alteration has come from the requirement of making the sensitivity uniform over a wide frequency range, which is considerably difficult to realize in a usual way on microwave frequency region. Multichannel system has also the possibility of recording the outputs of all the channels separately, which would be useful for precise discussions.

Fig. 2 is a simplified block diagram of the spectropolarimeter. First, two antennas receive two linearly polarized components perpendicular to each other, which are converted into two i-f signals at the mixers by a common swept-frequency local oscillator. The two i-f signals are amplified and led to a rat-race circuit where two linearly polarized components are converted into right- and left-hand circular components (hereafter to be called R and L). The R component is

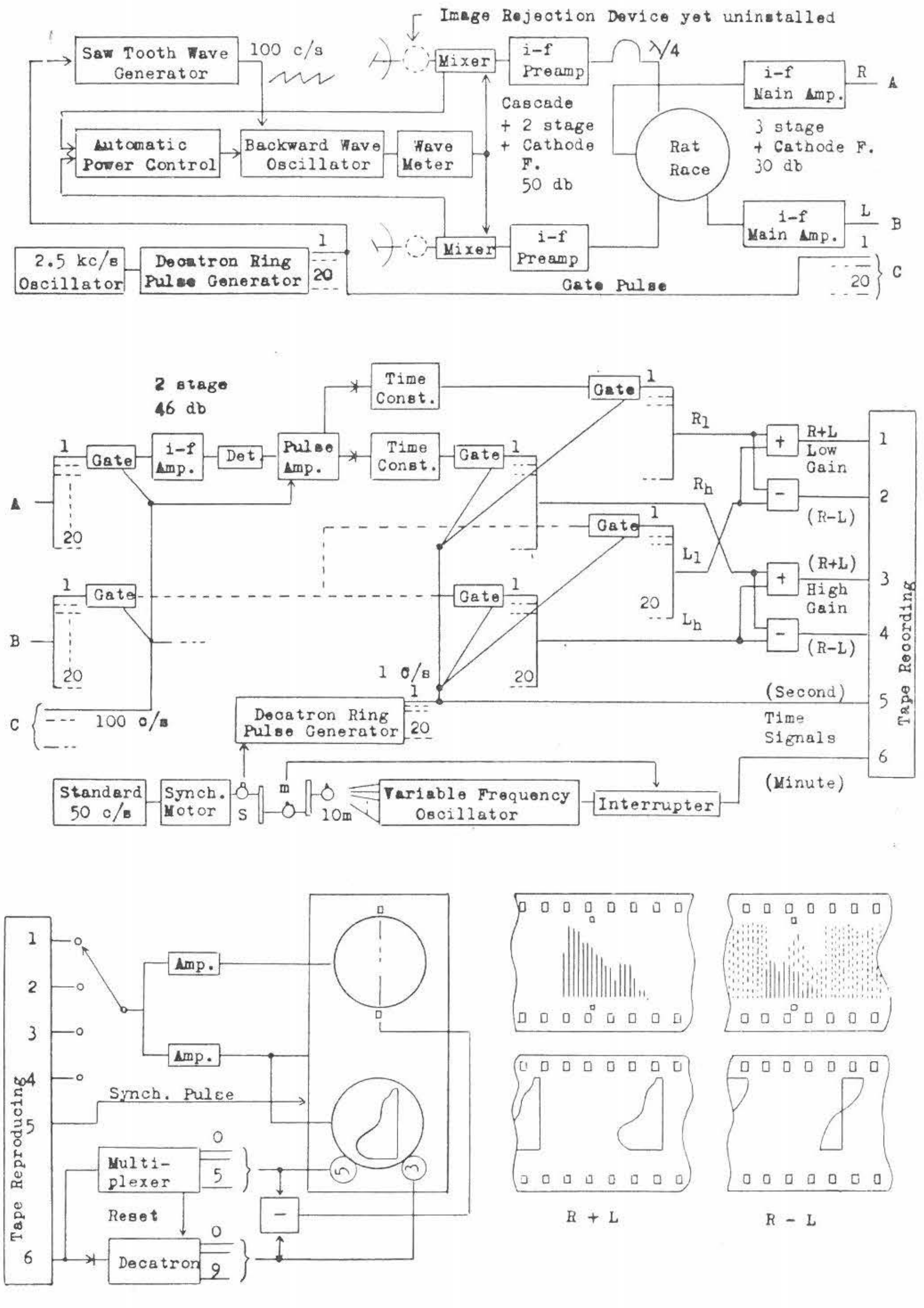

Fig. 2 Block diagram of the spectrometer.

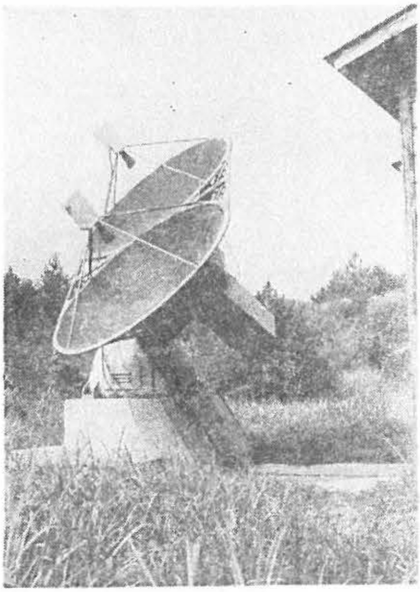

Fig. 3 General view of the antenna.

divided into 20 channels by going through time-division gates so that each channel takes a part of the total bandwidth of the receiver. Each i-f pulse signal is amplified and detected in a conventional way. The DC pulse thus produced is further amplified and rectified to make one of the 20 DC outputs. To avoid saturation, a continuous pulse train of constant amplitude is applied on the way of amplification for balancing out the basic noise. Twenty outputs are picked up one by one at a speed of one sweep per second to form a signal similar to that of a conventional spectrometer.

Another output of the rat-race circuit, or the L component, passes through similar circuits so that we have two kinds of swept-frequency signals each corresponding to R and L components. Then, after being added and subtracted, they are converted into the other two signals R+L and R−L, corresponding to the total flux density and the polarized component respectively. Additional 2 channels of R+L and R−L having lower sensitivity are prepared for large outbursts, and these 4 channels are led to the central receiver house where they are recorded on a magnetic tape together with time signals.

The tape recorder is of endless type. When a burst occurs, we take off the tape and reproduce the records afterwards. They are led to cathode-ray tubes one after another and are displayed on photographic films in two different ways. The one, as an intensity modulated film 35mm wide and the other, as a movie film of intensity spectrum, 16mm wide.

We did not notice until quite recently that two image signals on both sides of the local-oscillator frequency behave oppositely when we convert two linear components into circular ones after the frequency converters, i. e. when a signal is converted into R, the image signal is converted into L. So we have to reject one of the image signals for the present system, which is not so simple and is not yet realized. We are considering to change antenna feeds to receive two circular components directly, and for this purpose helical antenna seems to be hopeful.

3. Antenna

3. 1 Reflectors and Mounting

A twin reflector, each dish 2 meters in diameter, is mounted equatorially as shown

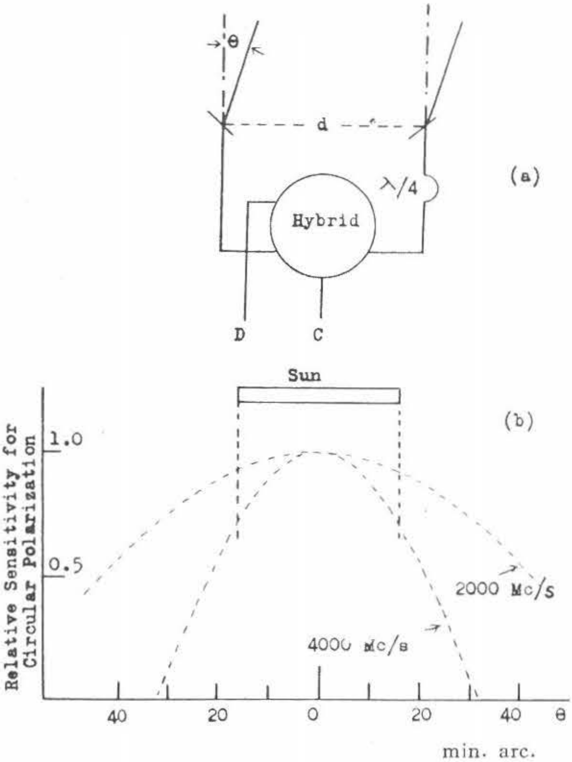

Fig. 4 Interference pattern for circularly polarized waves.

in Fig. 3. At the foci of 2 dishes, horn feeds are placed perpendicularly to each other. Following the feeds, crystal mixers and i-f pre-amplifiers are connected directly, and these assemblies are supported over the dishes symmetrically. The surface of the dishes is painted black to avoid the temperature rise of these assemblies. Two axies of the mount can be controlled either in the southern receiver cabin or in the central receiver house. The pointing accuracy is about 3 minutes of arc. The half-power width of the beam of each antenna is about 2.5° and 5° for 4000 and 2000 Mc/s respectively, which is broad enough to receive the total flux from the sun. These circumstances hold true also for twin dishes when the signal is randomly polarized, because there are no correlations between two inputs. For circularly polarized components, however, interference pattern plays the leading part.

Suppose the signal is circularly polarized in L sense. If the input of the antenna A in Fig. 4-a is unity, the input of B is exp. $i(\varphi+\pi/2)$, where $\varphi = (2\pi d/\lambda)\sin\theta$, θ is east-west angular deviation from the center axis. Then, after passing through a $\lambda/4$ section and a hybrid junction, the output at point C or L channel is $1+\exp.(i\varphi)$ and the output at D or R channel is $1-\exp.(i\varphi)$. The apparent percentage polarization is then $\cos\varphi$. This relation is shown in Fig. 4-b in terms of θ. It is seen from this figure that the relative sensitivity for circular polarization reduces by 30 percent at 4 Gc/s when a burst occurs at the extreme limb of the sun even when the antenna is correctly pointed to the sun.

The actual performance is more complicated, because the antenna pattern for polarized waves will fluctuate in a complex way owing to a possible phase error before the i-f hybrid junction. From an experiment made by putting a signal just in the middle of the antenna, it was found that the phase error changes from channel to channel having the maximum value of about 40 degrees, which is tolerable only for rough discussions. The difficulty discussed above will disappear when we receive 2 circular components directly at the antenna.

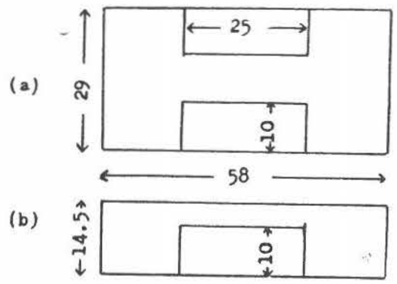

Fig. 5 Ridge waveguides.

3. 2 Antenna Feed

For wideband use, ridge waveguide[7] has been designed as shown in Fig. 5-a. It is composed of a standard waveguide with strips cut away from a brass sheet of 10mm thick. A waveguide of a half size shown in Fig. 5-b is also available, which is used at the mixer and at the throat of the horn feed. The size of the mouth of a feed, on the other hand, broadly determines the primary pattern.[8] It is designed here so that the field intensity comes about 10 db down at 2300 Mc/s or near the low frequency end of the receiving band. The shape of the horn is shown in Fig. 6-a. The impedance at infinite frequency is changing exponentially from the throat to the mouth. The measured VSWR is shown in Fig. 6-b, which is satisfactory for the present use.

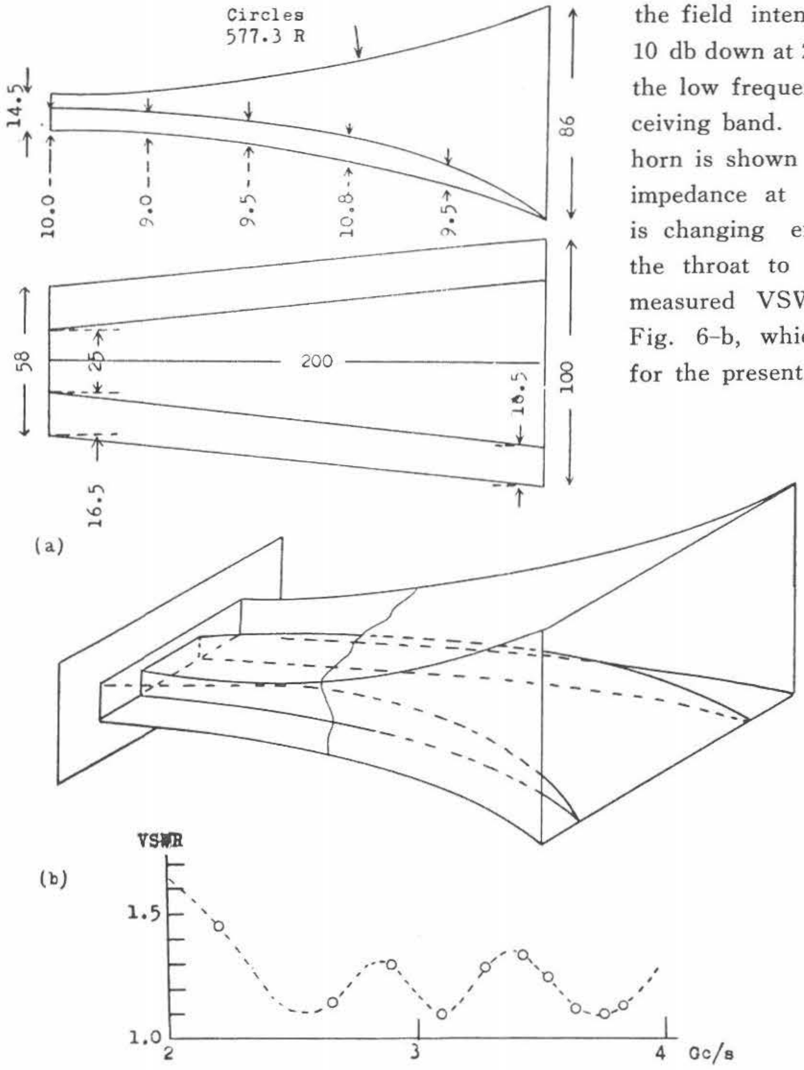

Fig. 6 Antenna feed.

4. Receiver

4. 1 Crystal Mixer

One of the most satisfactory mixers for wideband use may be the one shown in Appendix, and at first we planned to put the pair of this type behind the dishes. The mount of the antenna is designed to meet this requirement, though the boxes are now taken off as shown in Fig. 3. The main difficulty of using this type is that mechanical structure is too complicated to make the size of the pair completely equal including transmission lines. So we have looked for a simpler one at the sacrifice of conversion gain.

Fig. 7 is the mixer thus developed, which is similar to the step mixer.(9) The VSWR of this crystal mount is satisfactory, if not about 40 percent of power is consumed in the resistor. The most serious drawback of this mixer is that LO line has a poorly matched termination for wideband use and that it is awfully difficult to balance out the mixer pair over a wide frequency range. This makes also an important reason for having to choose multichannel system for this spectropolarimeter.

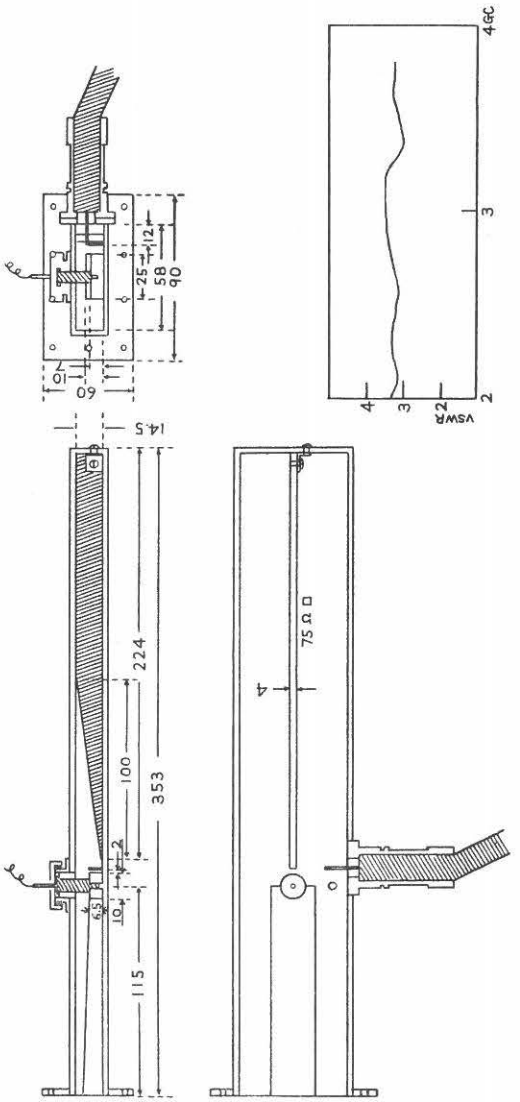

Fig. 7 Crystal mixer

4. 2 Local Oscillator

A backward-wave oscillator, Raytheon QK-518, is used as a swept-frequency oscillator. The frequency can be changed continuously from about 2 to 4 Gc/s by simply changing the delay line voltage from about 180 to 1500 volts. The maximum power is about 1 W near 4 Gc/s and about 0.1 W near 2000 Mc/s. The output power can be controlled by changing the grid voltage.

Fig. 8 is a block diagram of the local oscillator circuits and Fig. 9 is the details of transitions from coaxiale cable to waveguide.(10) To lighten the difficul-

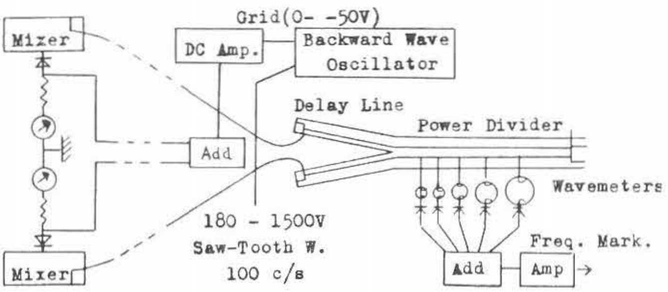

Fig. 8 Block diagram of the local oscillator circuits.

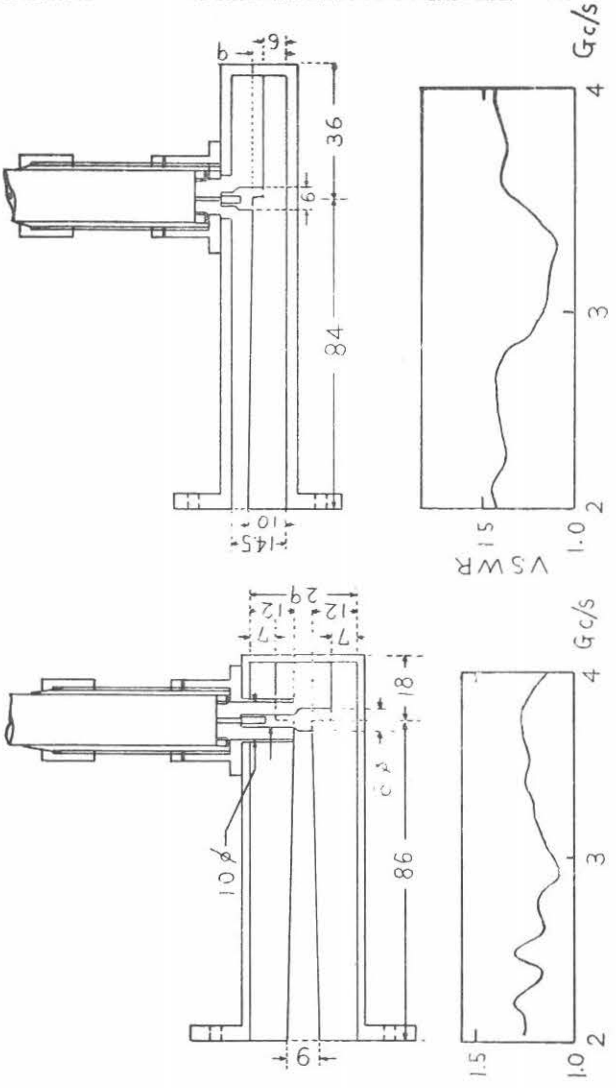

Fig. 9 Transitions from waveguides to coaxial cables.

ty of mismatch at the mixer, a long cable is inserted between the power divider and the mixer, i. e. a polyethylene cable 23 meters long. The loss of the cable is about 9 and 14.3 db for 2 and 4 Gc/s respectively. The worst VSWR at the nearest end of the cable may be then 1.3, which is tolerable for the power divider. The lossy cable is further useful not only for putting local oscillator assembly far apart from the mixer inside the receiver cabin but also to compensate partly the power change of oscillator with frequency. The grid of the oscillator tube is automatically controlled so that the mean value of two mixer currents remains constant. The actual performance of this LO assembly is satisfactory except that the output power is too small near the low frequency end; the available frequency is now limited between 2.5 to 4 Gc/s.

4.3 I-f Hybrid Junction and Power Distributor

A rat-race circuit(11) as shown in Fig. 10 is used as a hybrid junction for adding and subtracting two i-f signals. The performance is satisfactory for a required bandwidth of ±10 percent.

The output of the main i-f amplifier has to be branched into 20 cables. As it is not practical to connect all the cables together

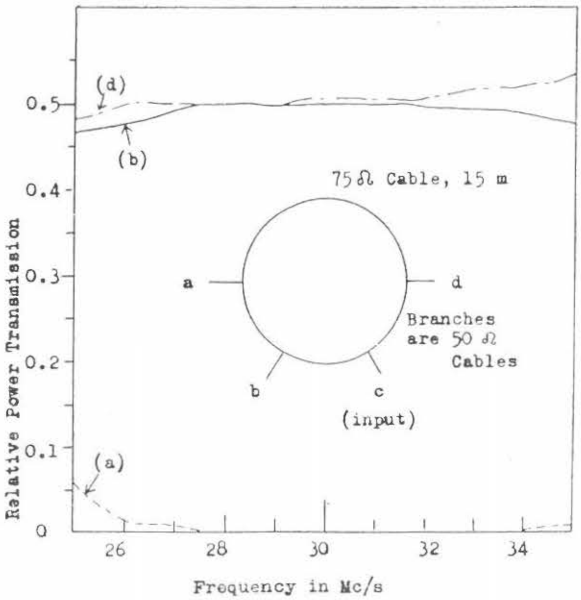

Fig. 10 Performance of rat-race hybrid ring.

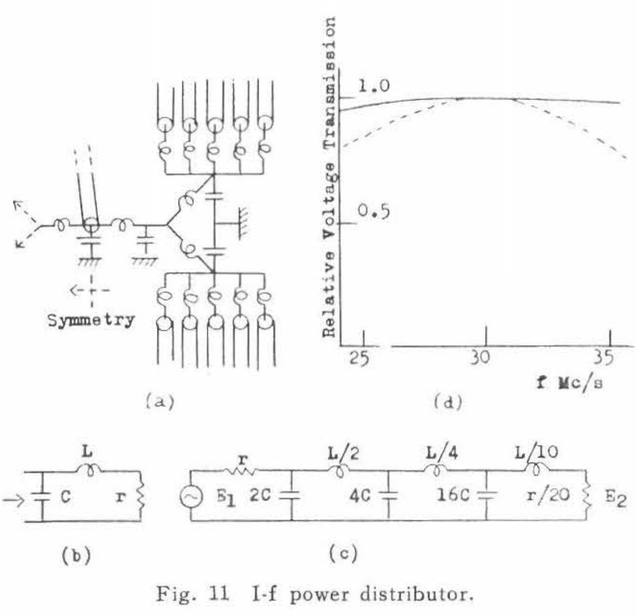

Fig. 11 I-f power distributor.

at a point, we have chosen a branch system as shown in Fig. 11-a. This is the combination of a simple impedance transformer shown in Fig. 11-b, where for n branches L and C are definitely fixed;

$$L=\sqrt{n-1}\, r/\omega_0,$$

$$C=\sqrt{n-1}\,/(n\omega_0 r).$$

The equivalent circuit of Fig. 11-a can be written as shown in Fig. 11-c, where the valuse of L and C are those for $n=2$, and r is the characteristic impedance of the cable. The voltage transfer function is calculated to be,

$$E_1/E_2=21-54x^2+29x^4-4x^6 +ix(28-30x^2+6x^4),$$

where $x=\omega/\omega_0$. This is plotted in Fig. 11-d as a solid line. The frequency characteristic is quite satisfactory and is much better than that using a one-step transformer as shown in the same figure. The real performance is close to the theoretical one, i. e. within ± 0.5 db for all channels over the required frequency band.

4. 4 Amplifier Unit

The circuit diagram of amplifier unit is shown in Fig. 12. One of the distributor branches enters a gating tube where a train of DC pulses synchronizing to the high-frequency sweep are applied; pulse separation is 10 ms and pulse width is 0.4 ms. The phase of pulses is shifted successively so as to cover the entire frequency band by 20 amplifier units. The gated i-f signal is amplified and detected into DC pulses in a usual way. Amplified DC-pulse signal is counterbalanced by a constant amplitude pulse signal to such an extent that about 1 volt remains when the antenna is directed towards the sky. The gain control just before this balanced

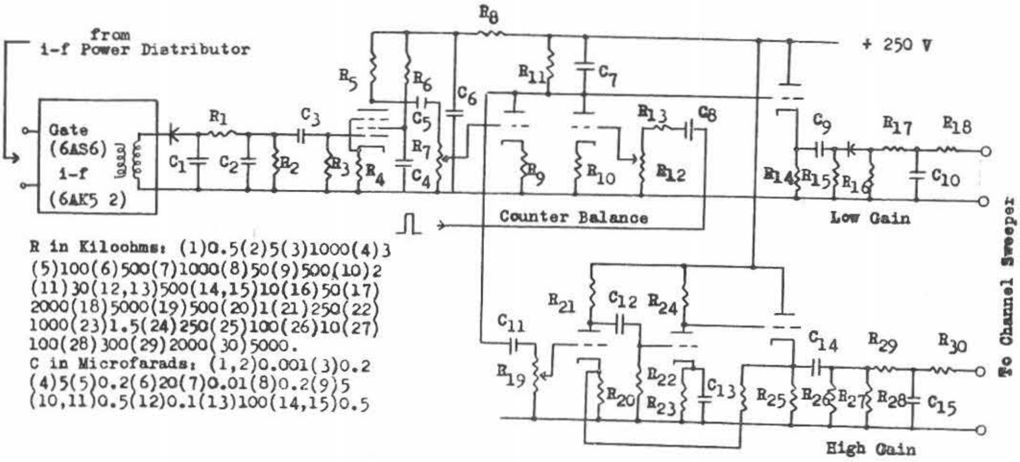

Fig. 12 Amplifier unit.

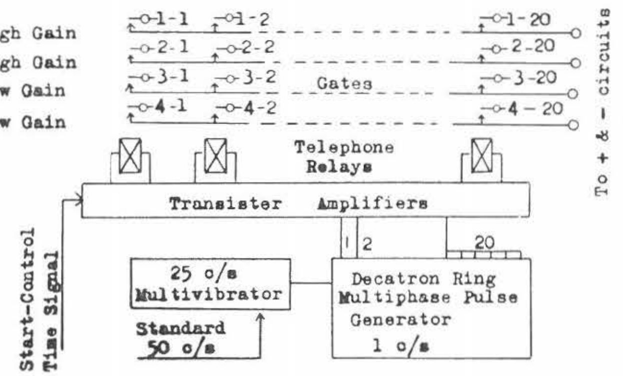

Fig. 13 Mechanical channel sweeper.

amplifier is adjusted to have the quiet-sun signal of about 0.5 volt. This signal is rectified by a diode after impedance transformation and is changed into DC signal similar to the output of a usual radiometer. The time constant is one second.

4. 5 Channel Sweeper

The difficulty of the channel sweeper lies in a high input impedance of the order of meg-ohms and a low voltage of the order of 1 volt. After many trials, the simplest relay system as shown in Fig. 13 was found to be most satisfactory. The guaranteed life of the miniature relay is $3\mathrm{x}10^7$ times, i. e. about 10^4 hours for the no-load use of 1 c/s.

A block diagram of the multiphase decatron-ring pulse generator is shown in Fig. 14. When the last element of a decatron tube fires, signal gate for the tube closes and at the same time the gate for the next tube opens to fire the first element, and so on. The same type of decatron-ring circuit is also used for producing i-f gate pulses.

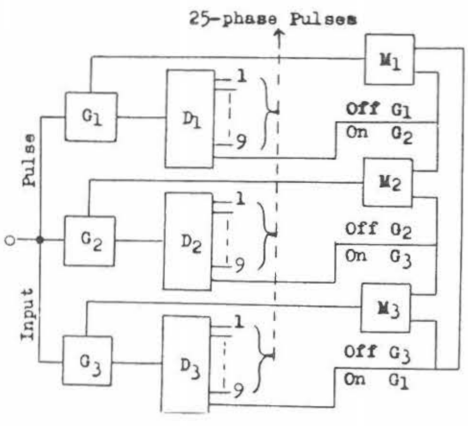

Fig. 14 Principle of decatron-ring multiphase Pulse generator.G: Gate, D: Decatron, M: Bistable Multivibrator.

4. 6 Time Signals

One of the recorder channels is exclusively used for the most important time signal, i.e. the synchronizing pulse of the low frequency sweep of 1 c/s. The phase of the pulse is fixed by the radio standard time signal when the equipment is first switched on.

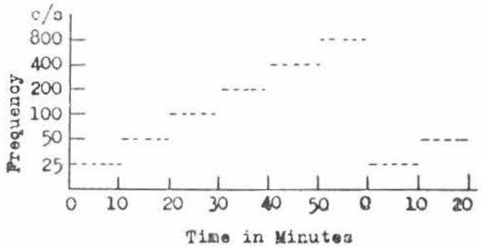

Fig. 15 Time signal for minutes.

The time signal for minutes is shown in Fig. 15, which is recorded on the other channel of the recorder. The frequency of the signal corresponds to the second order of minutes and the space of 0.1 seconds is inserted every minute. The signal, when reproduced, enters a multiplexer to select a figure on an indicator tube showing the second order of minutes. The same signal is rectified, on the other hand, to get one pulse per minute, which is sent to a decatron to show the first order of minutes on the other indicator tube. In this case, the figure on the indicator tube is indefinite until the frequency of the time signal changes for the first time.

For the intensity modulation display, only small spots are marked on both sides of the film every minute, with a missing spot every ten minutes.

4. 7 Magnetic Tape Recorder

A 6-channel tape recorder, Sony-TFR-3-6 has been used; all transistorized FM system with a frequency range from DC to 500 c/s (2 db). An additional recording mechanism has been prepared to make the recording endless. The endless system is shown in Fig. 16, where the end of each roll is detected by microswitches. When a burst alarm sounds, we replace the tape after the rewinding process.

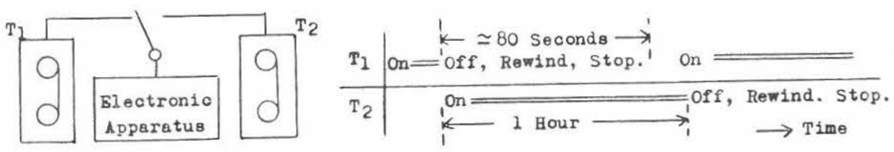

Fig. 16 Endless system of the tape recorder.

5. Over-All Performance

As we have few bursts on these days, we have yet only one record of a very small burst. Fig. 17 is the historical record taken on July 11, 1961. The maximum flux density was about 120×10^{-22} $WM^{-2}(c/s)^{-1}$. Time marks were bright lines at that time.

Over-all noise figure was measured using the sun as a signal. The value was different from channel to channel ranging from 12 to 16 db with the mean value of 14 db.

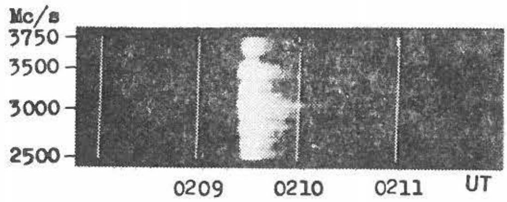

Fig. 17 Record of intensity spectrum on July 11, 1961.

The gain stability is not quite satisfactory on high gain channels, and it is necessary to adjust the counter-balance voltages twice a day to keep the minimum detectable flux density of about 50×10^{-22} $WM^{-2}(c/s)^{-1}$.

6. Future Problems

The first problem is to complete the polarization channels. The use of helical antenna seems to be more successful than trying to reject one of the image signals.

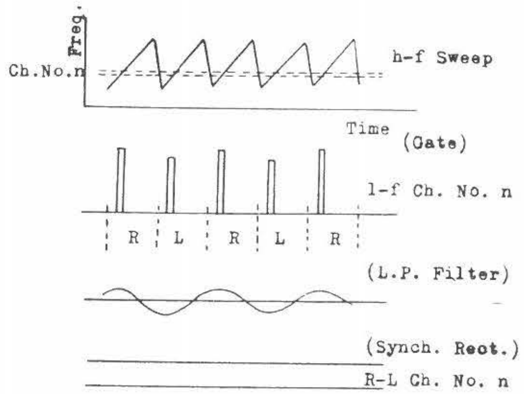

Fig. 18 Possible improvement for a polarization channel.

One of the weak points of this equipment is that R and L are amplified separately and so liable to suffer from gain variation. One possible improvement may be then as follows:— After the i-f gate, we can take R and L alternately as shown in Fig. 18. Then the Fourier component of a half the sweeping frequency is proportional to R∼L. So by using a selective amplifier and synchronous rectifier, we shall be able to get a DC output proportional to R∼L just like a radiometer using modulation method.

The method of display for polarization channels will have to be changed into a more convenient one, but it seems to be too early to discuss about this subject now.

References

(1) Tanaka, H. and Kakinuma, T.: Proc. Res. Inst. Atmospherics, Nagoya Univ., **4**, 60 (1956); **5**, 81 (1958).
(2) Tanaka, H.: ibid, **8**, 51 (1961).
(3) Tanaka, H. and Kakinuma, T.: ibid, **2**, 53 (1954); **3**, 102 (1955).
(4) Kakinuma, T. and Tanaka, H.: ibid, **8**, 39 (1961).
(5) Tanaka, H. and Kakinuma, T.: Proc. International Conf. Cos. Rays Earth Storms, Sup. to Jour. Phys. Soc. Japan (1962).
(6) Wild, J.P., Murray, J. D. and Rowe, W. C.: Austral. Journ. Phys., **7**, 439 (1954).
(7) Cohn, S.B.: Very-High-Freq. Techniques, 2, McGraw-Hill Book Co. Inc., 678 (1947).
(8) Risser, J.R.: M. I. T. Rad. Lab. Ser. **12**, 364 (1949).

(9) Soderman, R.A.: Very-High-Freq. Technique, 2, McGraw-Hill Book Co. Inc., 809 (1947).
(10) Ragan, G.L.: M. I. T. Rad. Lab. Ser. 9, 359 (1948).
(11) Dicke, R.H.: M. I. T. Rad. Lab. Ser. 8, 455 (1948).

Appendix

An Experiment of a Wideband Mixer

We first made an experiment of a wideband mixer as shown in Fig. 19. The fundamental idea was first published independently in three papers* at a time in 1953 as a

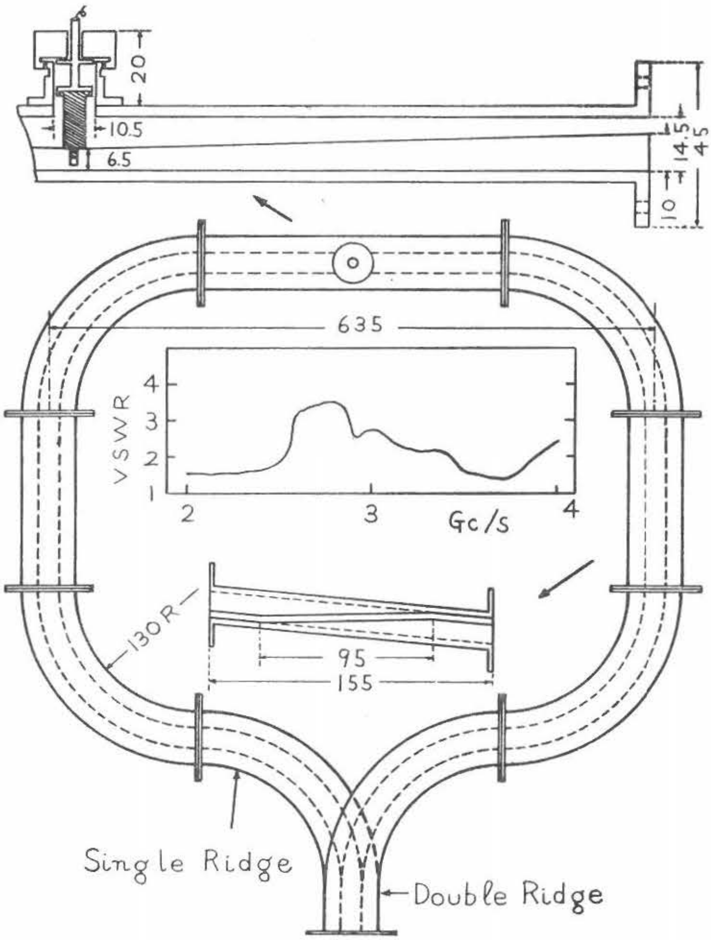

Fig. 19 A wideband mixer

* Nakano, M.: Preprints of the Joint Meeting of 4 Electrical Institutes in Japan, Oct. (1953), in Japanese. Tanaka, S.: ibid. Wheeler, H.A. and Spencer, N.A.: Convention Record of the I. R. E. National Convention, (1953).

wideband transition between waveguide and coaxial cable. This is the application of the same idea to the crystal mount. As the frequency band of 1 to 2 was aimed at, ridge waveguide was used which made the mechanical construction much more difficult. The VSWR shown in Fig. 19 was measured at the input terminal. It does not look much better than that shown in Fig. 7, but it must be remembered that in the latter case, about 40 percent of power is lost in the resistor.